Copper Transfer from Cu–Aβ to Human Serum Albumin Inhibits Aggregation, Radical Production and Reduces Aβ Toxicity

ARTICLE *in* CHEMBIOCHEM · JANUARY 2009

Impact Factor: 3.09 · DOI: 10.1002/cbic.200900474 · Source: PubMed

CHEMBIOCHEM

DOI: 10.1002/cbic.200900474

Copper Transfer from Cu–Aβ to Human Serum Albumin Inhibits Aggregation, Radical Production and Reduces Aβ Toxicity

Lorena Perrone,[a, b] Emmanuelle Mothes,[c, d] Maeva Vignes,[c, d] Anaïs Mockel,[a, b] Cindy Figueroa,[c, d] Marie-Christine Miquel,[a, e, f] Marie-Lise Maddelein,[a, b] and Peter Faller*[c, d]

Amyloid-β peptides (Aβ) and the protein human serum albumin (HSA) interact in vivo. They are both localised in the blood plasma and in the cerebrospinal fluid. Among other functions, HSA is involved in the transport of the essential metal copper. Complexes between Aβ and copper ions have been proposed to be an aberrant interaction implicated in the development of Alzheimer's disease, where Cu is involved in Aβ aggregation and production of reactive oxygen species (ROS). In the present work, we studied copper-exchange reaction between Aβ and HSA or the tetrapeptide DAHK (N-terminal Cu-binding domain of HSA) and the consequence of this exchange on Aβ-induced ROS production and cell toxicity. The following results were obtained: 1) HSA and DAHK removed Cu^{II} from Aβ rapidly and stoichiometrically, 2) HSA and DAHK were able to decrease Cu-induced aggregation of Aβ, 3) HSA and DAHK suppressed the catalytic $HO^{\bullet}$ production in vitro and ROS production in neuroblastoma cells generated by Cu–Aβ and ascorbate, 4) HSA and DAHK were able to rescue these cells from the toxicity of Cu–Aβ with ascorbate, 5) DAHK was more potent in ROS suppression and restoration of neuroblastoma cell viability than HSA, in correlation with an easier reduction of Cu^{II}–HSA than Cu–DAHK by ascorbate, in vitro. Our data suggest that HSA is able to decrease aberrant Cu^{II}–Aβ interaction. The repercussion of the competition between HSA and Aβ to bind Cu in the blood and brain and its relation to Alzheimer's disease are discussed.

Introduction

Extracellular amyloid plaques and intracellular neurofibrillary tangles are the two main morphological hallmarks of Alzheimer's disease (AD).[1–3] Amyloid plaques contain aggregated forms of the 39–43 amino acid amyloid-β peptide (Aβ). Aβ is strongly implicated as a causative factor responsible for the development of AD. According to the amyloid cascade hypothesis,[4,5] an increased Aβ production and/or accumulation lead first to the formation of Aβ oligomers, then to protofibrils and ultimately to fibrils, which are the main constituent of the amyloid plaques.[6] These oligomers are now supposed to be the most (but not exclusive) toxic species responsible for neuronal dysfunction and ultimately death. Several mechanisms for Aβ toxicity have been proposed.[7] One of these mechanisms includes the production of reactive oxygen species (ROS) by the aberrant binding of redox active copper ions to Aβ.[8–10] Copper has been found at high concentration in amyloid plaques and bound to Aβ.[11–13] Copper(II) binds to Aβ with an apparent K_d of about 0.1 to 1 nM (in aqueous solution (no buffer) at pH 7.4;[14] for a recent review see ref. [15]) and modulates the aggregation behaviour.[16] Moreover, Cu^{II} can potentiate the Aβ toxicity in cell culture.[17] Cu^{II} is bound to Aβ in a ratiometric and monomeric Cu^{II}_1–$Aβ_1$ complex prior to aggregation.[18] The mononuclear Cu^{II} site is maintained during aggregation.[19,20] Cu^{II}_1–$Aβ_1$ is a very dynamic complex, including different Cu binding modes to Aβ. There is still ambiguity concerning the most populated coordination mode, but it is clear that the amino acids His6, -13, -14 and Asp1 are involved in Cu binding around neutral pH (for recent publications see refs. [21] and [22]; for recent review see ref. [15]). In agreement with the production of ROS by Aβ and cellular toxicity of Aβ oligomers compared to monomers, we and others have found that Cu–Aβ complexes can produce ROS catalytically in the presence of a physiological reductant (e.g., ascorbate, VitE).[23–27] Moreover, intermediates of the aggregation process

[a] Dr. L. Perrone, A. Mockel, Dr. M.-C. Miquel, Dr. M.-L. Maddelein
CNRS UMR 5089, IPBS (Institut de Pharmacologie et de Biologie Structurale)
205 route de Narbonne, 31077 Toulouse (France)

[b] Dr. L. Perrone, A. Mockel, Dr. M.-L. Maddelein
Université de Toulouse, UPS, IPBS, 31077 Toulouse (France)

[c] E. Mothes, M. Vignes, C. Figueroa, Prof. Dr. P. Faller
CNRS, LCC (Laboratoire de Chimie de Coordination)
205, route de Narbonne, 31077 Toulouse (France)
Fax: (+33) 561553003
E-mail: peter.faller@lcc-toulouse.fr

[d] E. Mothes, M. Vignes, C. Figueroa, Prof. Dr. P. Faller
Université de Toulouse, UPS, INPT, LCC, 31077 Toulouse (France)

[e] Dr. M.-C. Miquel
Present address: UMR5241 Métabolisme, Plasticité et Mitochondrie
118 Route de Narbonne, 31400 Toulouse (France)

[f] Dr. M.-C. Miquel
UPMC, 75005 Paris (France)

Supporting information for this article is available on the WWW under http://dx.doi.org/10.1002/cbic.200900474.

(oligomers) showed a higher generation of ROS than monomers or larger aggregates.[23,24]

Human serum albumin (HSA; 66.5 kDa) is the most abundant protein in blood plasma and in cerebrospinal fluid (CSF) with typical concentrations of ~0.6 mM and ~4 μM, respectively. HSA constitutes 35–80% of the total proteins in CSF.[28] HSA has been proposed to be involved in metal ion transport and has a variety of metal sites with different specificities.[29–33] The best characterized metal site of HSA is the one binding Cu^{II} (and Ni^{II}). These metal ions bind strongly with a square planar geometry to four nitrogen ligands from Asp1-Ala2-His3 at the N terminus (Scheme 1). Cu^{II} has an apparent K_d (aqueous solution at pH 7.4 and no buffer) of ~1 pM.[34,35] The tetrapeptide DAHK (Asp1-Ala2-His3-Lys4) has been often used as a model for the N-terminal Cu^{II} and Ni^{II} binding site of HSA. Such a complex can be formed with all peptides/proteins having an N-terminal sequence of Xxx-Xxx-His (where Xxx is any amino acid but Pro). This binding motif exists in different native peptides/proteins and was dubbed the amino terminal Cu^{II}, Ni^{II} binding (ATCUN) motif (for review see ref. [36]); NMR spectroscopy and crystallographic data have provided the molecular structure of the ATCUN motif[29,37] (Scheme 1).

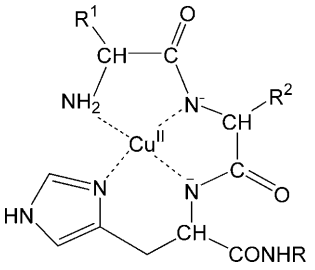

Scheme 1. Structure of the ATCUN motif found in Cu^{II}–DAHK and Cu^{II}–HSA (R: rest of protein, R^1: Asp, R^2: Ala).

Although Cu^{II}–HSA is the major transport form of copper in the blood, only 5–10% of serum copper is bound to HSA; most of the copper is bound to ceruloplasmin, which binds Cu^{II} strongly and does not transfer it further, and to peptides and amino acids (mostly histidines).[36] HSA in the blood is only partially (about 4%) complexed with copper(II), that is, the majority of the N-terminal binding site is not occupied by metal ions.[38] Although the occupancy level of HSA by Cu in the CFS is not known, it might be in the same range or higher considering that HSA crosses the blood–brain barrier (BBB) by a receptor-independent mechanism (passive diffusion)[39] and that the general Cu content in the brain is at least one order of magnitude higher than in the blood.[40] Moreover, HSA and DAHK have been shown to block neuronal death induced in vitro by H_2O_2 or $CuCl_2$/ascorbate in cell culture.[41]

Aβ is also found in the blood plasma, where it is mainly bound to HSA (~90%).[42] In vitro, Aβ can bind stoichiometrically to HSA with an apparent dissociation constant of ~5 μM.[43,44] This interaction inhibits the polymerisation of Aβ.[44] So it is clear that HSA and Aβ interact and copper transfer might occur in the plasma. Even if interaction of HSA and Aβ in CSF or brain tissue has not been shown, the presence of both molecules in the CSF suggests that a copper-transfer reaction should be physiologically relevant. Noteworthy, HSA might protect Aβ from aberrant copper binding in brain since its concentration in the CSF is more than two orders of magnitude higher than that of Aβ.[45] Moreover, this protective effect might be impaired in Alzheimer's disease as it has been shown that permeability of HSA across the BBB is decreased in AD model mice,[46] while Aβ concentration is increased in AD brains.[2,5] In addition, copper removal from Aβ by chelators (also called metal–protein attenuating compounds or MPAC) seems to be a promising strategy for Alzheimer's therapy as MPAC were reported to reduce brain amyloid concentrations, plaque burden and attenuate cognitive decline.[47–52]

In the present study, we investigated the copper-transfer reactions between Aβ and HSA as well as its Cu-binding domain DAHK. In particular, we assessed the relative Cu^{II}-binding affinity between the two molecules as well as the effect of HSA on Cu-induced aggregation, ROS production and toxicity on neuroblastoma cells.

Results

Cu^{II} transfer from Aβ40 to HSA

X-band electron paramagnetic resonance (EPR) was used to follow Cu^{II} transfer from Aβ40 peptide to HSA. The EPR spectra of Cu^{II}–Aβ40 and Cu–HSA are quite different[20,53–55] (Figure 1). Upon titrating HSA to Cu^{II}–Aβ, the EPR spectrum changed steadily towards the typical spectrum of Cu^{II}–HSA up to one equivalent. Addition of more HSA did not change the spectrum further. This result indicates that Cu^{II} is transferred quantitatively to HSA and hence the affinity of Cu^{II} for HSA is substantively higher than for Aβ40. This Cu transfer can best

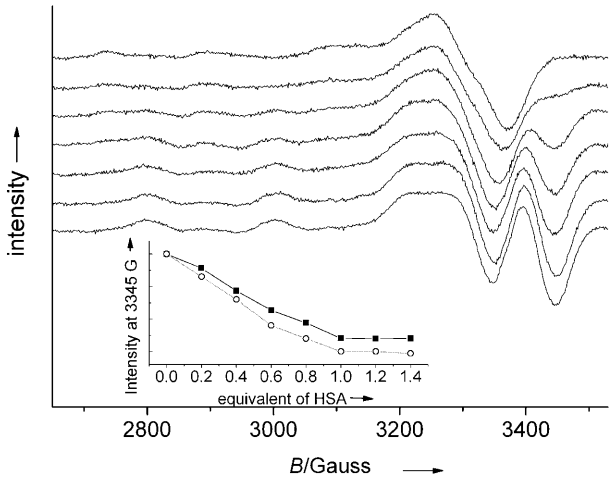

Figure 1. EPR spectra of the titration of HSA to Cu^{II}–Aβ40. From top to bottom the spectra represent the addition of 0, 0.2, 0.4, 0.6, 0,8, 1.0 and 1.2 equiv HSA per Cu^{II}_1–Aβ40. Conditions: 100 μM Aβ40, 80 μM $Cu^{II}Cl_2$ in 40 mM HEPES, pH 7.4, 100 mM NaCl; temperature 100 K, power 1 mW. Inset: change of peak intensity at 3345 Gauss during the titration of HSA to Cu^{II}–Aβ40 (■) and for titration of HSA to Cu^{II}–Aβ16 (○).

be followed by the appearance of a negative peak at 3445 Gauss (Figure 1) present in Cu^{II}–HSA but not in Cu–Aβ40. The development of this peak increased steadily in intensity up to the addition of one equivalent of HSA, where a plateau is reached (Figure 1, inset). This result is in agreement with the estimated apparent K_d values of 1 pM and ~10–1000 pM for HSA (or its binding domain DAHK) and Aβ, respectively.[15,35,56]

Cu^{II} transfer from Aβ16 to HSA

The truncated Aβ16 peptide containing the first 16 amino acids of the full-length Aβ has been shown to contain the metal-binding sites.[15,20–22,55,57–59] We investigated Cu^{II} transfer from Aβ16 to HSA by EPR (Figure 1, inset) and by electronic absorption (see the Supporting Information). Like Aβ40, HSA was able to withdraw Cu^{II} from Aβ16 quantitatively. Experiments with Aβ16 were facilitated because this truncated peptide does not spontaneously aggregate and should not interact with HSA by peptide/protein interaction, since it does not contain the hydrophobic part of the Aβ40 supposed to interact with HSA.[60] As a consequence, the use of Aβ16 allowed the confirmation of Cu transfer under nonaggregating conditions and in the absence of a complex Aβ–HSA.

HSA and DAHK reversed Cu^{II}-induced aggregation of Aβ40

Since the above data suggest that HSA is able to capture Cu^{II} from Aβ almost stoichiometrically, the next question was whether HSA and DAHK are able to reverse Cu^{II}-induced aggregation of Aβ40. Several methods were applied. First, an approximate assay of turbidity was used. As shown in Figure 2, addition of 1 equiv Cu^{II} induced a fast increase in turbidity

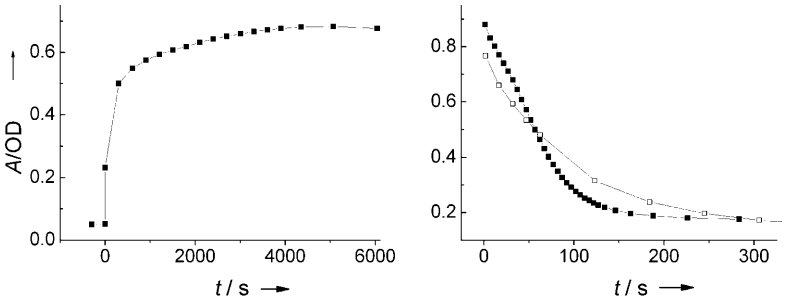

Figure 2. Turbidity of Aβ40 at 400 nm. Left-hand panel: turbidity of 100 μM Aβ40 (before $t=0$) and change upon addition of 1 equiv Cu^{II} at $t=0$. Right-hand panel: Cu–Aβ40 from the left panel (incubation for about 2 h) upon addition of 1 equiv HSA (■) or DAHK (□) at $t=0$.

during the first five minutes. After about 50 min the turbidity level reached a plateau. Following the addition of 1 equiv HSA or DAHK, the turbidity level decreased rapidly (about three to five minutes) and returned to the basic level observed before Cu addition. These data indicate that HSA and DAHK are able to reverse Cu-induced aggregation of Aβ.

To further confirm that HSA and DAHK are able to revert Cu-induced aggregation of Aβ40, the amounts of monomeric Aβ before and after addition of HSA were estimated by separation on size-exclusion chromatography (SEC).[18] The monomeric peak observed after Cu^{II} addition doubled in size after addition of HSA; this indicates that HSA was able to resolubilize Aβ40 aggregates formed in the presence of Cu (Figure 3). The monomeric Aβ was quantified based on the known absorption at 275 nm for Aβ40 (see, e.g., ref. [59]). This quantification revealed that before HSA addition 17% of Aβ was in a monomeric state, and after addition of 1 equiv HSA, the monomeric Aβ fraction increased to 32%, in line with a partial monomerisation of the Cu^{II}–Aβ40 aggregates by HSA. DAHK showed similar results (see the Supporting Information). Note that the fraction of monomeric Aβ without HSA is overestimated because Cu binding to Aβ increases the absorption at 275 nm as the extinction coefficient is higher after Cu binding. Moreover, no peaks corresponding to aggregates were detected on the chromatogram with or without HSA; this indicates that the aggregates were too large to enter the column and/or too heterogeneous to be detected.

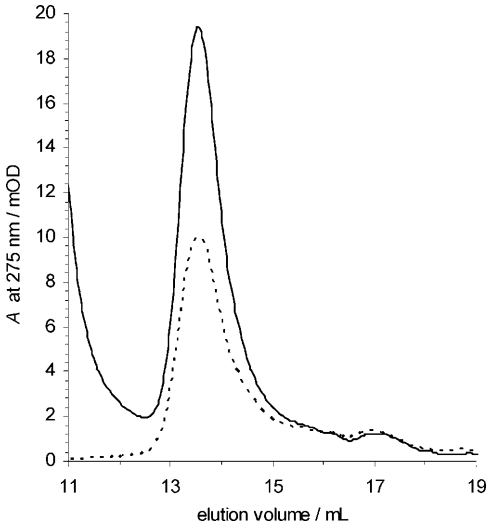

Figure 3. Size-exclusion chromatography of Cu–Aβ40 before (····) and after (——) addition of HSA; absorption at 275 nm.

Transmission electron microscopy (TEM) was used to determine the type of aggregates formed (Figure 4).[1] Aβ40 alone, after sample preparation, showed very little nonfibrillar aggregation (data not shown). After four days incubation, aggregates were observed along with fibrils (Figure 4A). Cu–Aβ40, showed more aggregates than Aβ40 alone, and the amount of aggregated material increased after four days incubation (Figure 4B, note that sample was diluted 20 times). However, no fibrillar struc-

[1] *Samples were first analysed at the same concentration (100 μM) as for the turbidity experiments. These high concentrations on the grids made it difficult to see individual structures, but generally it confirmed that HSA is able to reverse Cu-induced aggregation.*

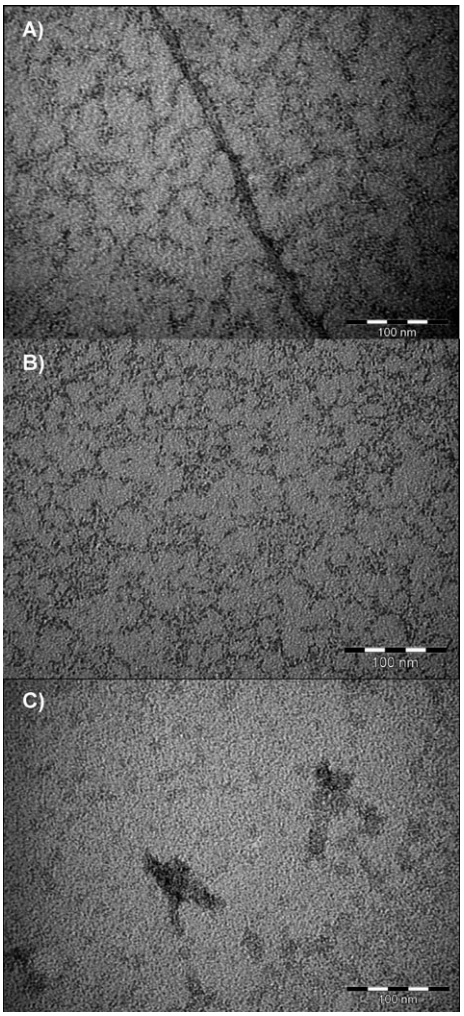

Figure 4. Transmission electron microscopy: 20 μM Aβ40 after four days incubation in 20 mM HEPES, pH 7.4, 100 mM NaCl. A) Aβ alone; B) Cu–Aβ40, 20-times diluted, and C) Cu–Aβ40 with HSA; scale bars correspond to 100 nm.

tures could be observed under this condition. These observations are in line with the report by Smith et al.[61] Upon addition of HSA (Figure 4C), Cu–Aβ40 solution contained few aggregates (even after four days of incubation) and no fibrils were observed.

TEM measurements confirmed the turbidity and SEC analysis, indicating that HSA can resolubilise, at least partially, Cu-induced Aβ aggregates. However, TEM images of Cu–Aβ aggregates differ from those of Aβ aggregates—the former contain more amorphous-like aggregates.

Measurement of hydroxyl radical production

Many reports indicate that Cu–Aβ complexes could be directly involved in the generation of oxidative stress leading to neuronal degeneration (for reviews see, e.g., refs. [9] and [62]). Recently, we have shown that Cu^{II}–Aβ is able to generate substantial amount of HO• in the presence of ascorbate under aerobic conditions.[23] These conditions were chosen because the brain is well supplied with oxygen and ascorbate is available at high concentrations in brain cells (neuron 10 mM, glia 1 mM). In addition, extracellular ascorbate is quite abundant: concentrations of 500 μM in the cerebrospinal fluid and 200–400 μM in extracellular fluid have been reported.[63] The Cu and Zn binding protein metallothionein-3 (MT-3) has been shown to be able to suppress the production of HO• under these conditions.[64] Therefore, we used the same methods to determine the capacity of HO• production by Cu–HSA and Cu–DAHK. HO• production was followed by fluorescence by using HO• trapping agent coumarin-3 carboxylic acid (CCA;[23] Figure 5). As reported earlier,[23] "free" Cu in the buffer generated the highest amount of HO• and was used as reference (100%). Cu–Aβ (Aβ40 and truncated Aβ16) showed about 16% HO• production compared to "free" Cu, in agreement with our previous observation.[23] These experiments have been recently confirmed.[65] We observed that addition of either HSA or DAHK abolished HO• production from Cu–Aβ (Figure 5, upper panel). Cu–DAHK did not produce significant amount of HO• in line with the literature,[23,66] and neither did Cu–HSA (< 2%). In

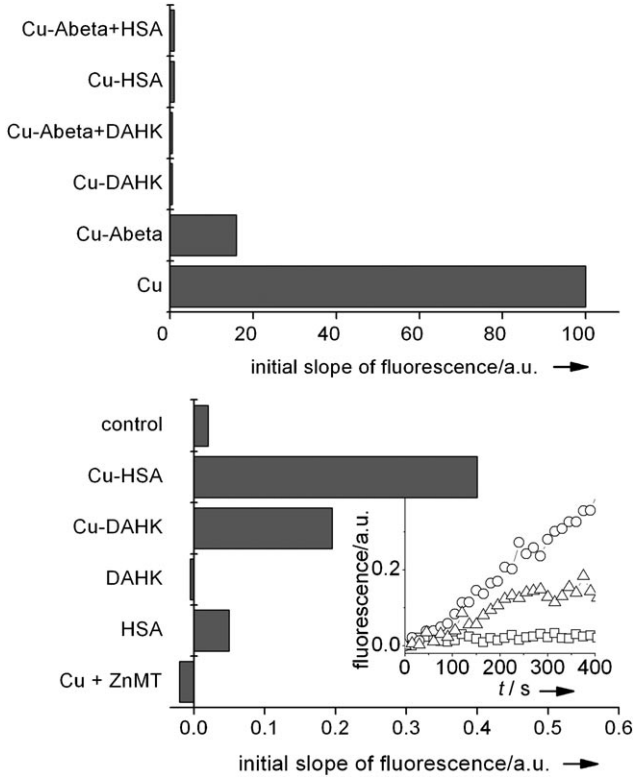

Figure 5. Upper panel: HO• generation of different Cu complexes. HO• formation was followed by fluorescence detection of 7-hydroxycoumarin carboxylic acid formed by the treatment of HO• with 3-coumarin carboxylic acid (excitation wavelength: 395 nm; emission wavelength: 450 nm). The initial inclination of the fluorescence intensity of 7-HO-coumarin-3-carboxylic acid for different Cu complexes was measured to the initial inclination of free Cu^{II}. Conditions: Cu complexes (10 μM), ascorbate (300 μM), desferiooxamine (1 μM), CCA (1 mM) in PBS buffer, pH 7.4. Lower panel (main graph): HO• generation at the following conditions: Cu (80 μM), DAHK or HSA (100 μM), MT-3 (50 μM), ascorbate (0.6 mM), deferoxamine (1 μM), coumarin-3-carboxylic acid (CCA; 1 mM) in PBS buffer, pH 7.4. Inset: initial slope of fluorescence intensity of Cu–HSA (○), Cu–DAHK (△), and the control (□; without any Cu complex).

order to increase the assay sensitivity, measurements were repeated by using higher concentrations of Cu–protein/peptide and ascorbate (Figure 5, lower panel). Both complexes produced significant HO•, with about a twofold production from Cu–HSA compared to DAHK (about 1.2 and 0.5%, respectively, compared to our standard "free Cu"). In absence of Cu, DAHK produced clearly no significant amount of HO•, whereas HSA might produce very little in line with its partial (~4%) Cu load (accuracy of the method in Figure 5B is considered to be ±0.03). For comparison, MT-3 was measured under the same conditions. This protein has been shown in the past to be able to suppress HO• production and to protect neuroblastoma cells from Cu–Aβ toxicity.[64,67] Cu–MT-3 did not produce any significant amount of HO• (Figure 5, lower panel). This corroborates the result that the Cu bound to HSA and DAHK produce little but significant amounts of HO•, and that Cu–HSA produces significantly more HO• than DAHK.

Based on the observations that: 1) DAHK and HSA retrieve Cu^{II} from Aβ almost completely, and 2) that chelation of Cu^{II} by DAHK and HSA led to a strong decrease of HO• production, DAHK and HSA should be able to suppress HO• generation by Cu–Aβ. Indeed, the addition of an equimolar amount of DAHK or HSA to Cu–Aβ almost completely suppressed HO• (Figure 5, upper panel).

To summarise, chelation of Cu by DAHK or HSA almost completely abolished the capacity of HO• generation in the presence of ascorbate and oxygen, DAHK being more efficient than HSA.

Reduction of Cu^{II}–DAHK and –HSA by ascorbate

In order to obtain insight into the difference of HO• generation by Cu–DAHK and Cu–HSA, an attempt to measure the redox potentials of Cu–HSA by cyclic voltammetry was undertaken, as it has been done for Cu–DAHK.[23] However, no signal for Cu–HSA could be detected, perhaps because HSA is a large molecule and has hence a low diffusion coefficient. In case of adsorption on the electrode, the Cu site could be too far away from the electrode to allow efficient electron transfer.

We then compared the capability of ascorbate to reduce Cu^{II} bound to DAHK or to HSA. Figure 6 shows the d–d bands of Cu^{II} in Cu–HSA (left panel) and Cu^{II}–DAHK (right panel). Upon addition of ascorbate under anaerobic conditions (to avoid the production of reactive radical species) the d–d band diminished in the case of Cu–HSA but not for Cu–DAHK. This suggest that ascorbate is able to reduce Cu^{II} to Cu^{I} in HSA but not in DAHK. This result also correlates with the higher formation of HO• by Cu–HSA than Cu–DAHK as the redox cycling $Cu^{II/I}$ is the underlying mechanism of HO• formation.

SH-SY5Y cell toxicity

As shown above, DAHK and to a slightly lesser extend HSA were able to strongly decrease the production of HO• by Cu–Aβ in the presence of ascorbate. To see whether or not HSA or DAHK are able to protect cells from Cu–Aβ induced toxicity, viability assays were conducted on neuroblastoma SH-SY5Y cells (Figure 7). We used the same conditions as in our previous studies, in which MT-3 had a marked protective effect (restoration of 80% cell viability).[64] Incubation of SH-SY5Y cells for 24 h in 40 μM Cu–Aβ and 300 μM ascorbate significantly reduced cell viability to about 10% ($p < 0.001$) in agreement with our previous results.[64] Addition of a stoichiometric amount of DAHK increased cell viability modestly but with statistic significance ($p < 0.05$), however, addition of a

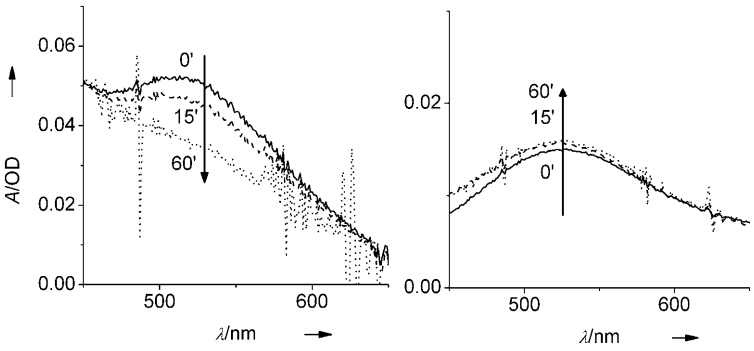

Figure 6. Reduction of Cu^{II}–HSA (left) and Cu^{II}–DAHK (right) by ascorbate estimated from the d–d bands. Conditions: 10 mM ascorbate, 0.5 mM HSA with 0.7 equiv Cu and 0.1 mM DAHK with 0.8 equiv Cu in 40 mM HEPES, pH 7.4, 100 mM NaCl; anaerobic conditions.

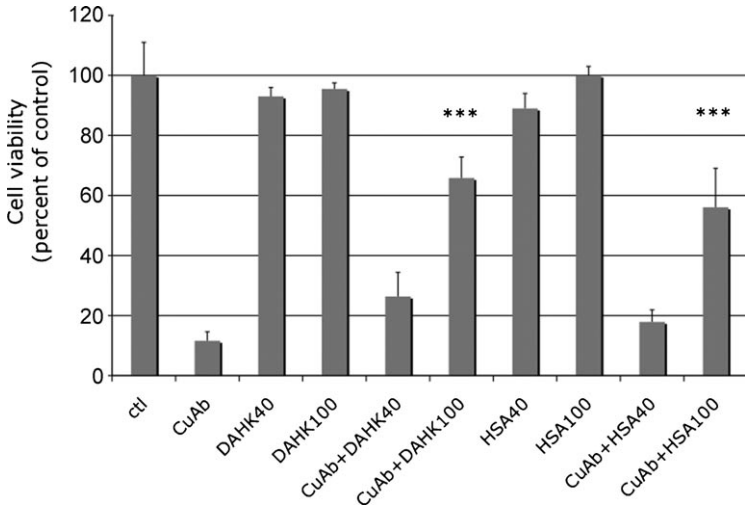

Figure 7. Effect of Cu^{II}–Aβ40, DAHK and HSA on the survival of SH-SY5Y neuroblastoma cells determined with the MTT assay. Ctl: control (300 μM ascorbate, absence of Aβ, Cu, HSA and DAHK); CuAb: addition of 40 μM Cu^{II}–Aβ40; DAHK40: addition of 40 μM DAHK; DAHK100: addition of 100 μM DAHK; CuAb + DAHK40: addition of 40 μM Cu^{II}–Aβ40 and 40 μM DAHK; CuAb + DAHK100: addition of 40 μM Cu^{II}–Aβ40 and 100 μM DAHK; HSA40: addition of 40 μM HSA; HSA100: addition of 100 μM HSA; CuAb + HSA40: addition of 40 μM Cu^{II}–Aβ40 and 40 μM HSA; CuAb + HSA100: addition of 40 μM Cu^{II}–Aβ40 and 100 μM HSA. All experiments were performed in the presence of 300 μM ascorbate. ANOVA test: *** = $p < 0.001$ between Cu^{II}–Aβ40 and Cu^{II}–Aβ40 plus 100 μM DAHK or 100 μM HSA.

stoichiometric amount of HSA did not. At a higher concentration (2.5 equiv per Cu–Aβ; $p < 0.001$) both HSA and DAHK increased cell viability significantly. These results suggest that: 1) DAHK and HSA can partially rescue SH-SY5Y cells from Cu–Aβ toxicity, 2) DAHK has a higher potential to rescue the cells than HSA.

Intracellular ROS production in SH-SY5Y cells

The ability of HSA and DAHK to decrease cell toxicity of Cu–Aβ seemed to correlate with their respective capacity to abolish HO• production from Cu–Aβ, in vitro. These findings are in agreement with previous observations that Aβ-induced cell death is mediated by ROS production (see, e.g., refs. [68] and [69]). To get better insight and to determine whether HSA and DAHK are able to decrease oxidative stress in neuroblastoma cells, intracellular ROS production was monitored by using the fluorescent dye 2′,7′-dichlorodihydrofluorescein diacetate (H_2DCFDA) in SH-SY5Y cells.

We observed that Cu–Aβ in the presence of ascorbate showed a significant ($p < 0.001$) increase in DCF fluorescence compared to the control cells and to Aβ addition in the absence of copper and ascorbate (Figure 8). We observed a dose–response reduction of Aβ-induced ROS production in SH-SY5Y cells by HSA or DAHK. DAHK was a more potent suppressor of intracellular ROS production at the same concentration compared to HSA (Figure 8). Indeed, 40 μM addition of HSA to the mixture of Aβ, copper and ascorbate still showed a significant production of intracellular ROS compared to Aβ addition to cells in the absence of copper and ascorbate. On the contrary, 40 μM addition of DAHK restored intracellular ROS production to a similar level as induced by Aβ alone in the absence of copper and ascorbate addition (Figure 8). These results correlate clearly with in vitro suppression of HO• production by HSA/DAHK and the cell viability experiments; this indicates that HSA and DAHK might rescue SH-SY5Y cells by inhibiting Cu–Aβ catalyzed ROS production. In all three experiments, DAHK had the tendency to be a better inhibitor/protector than HSA.

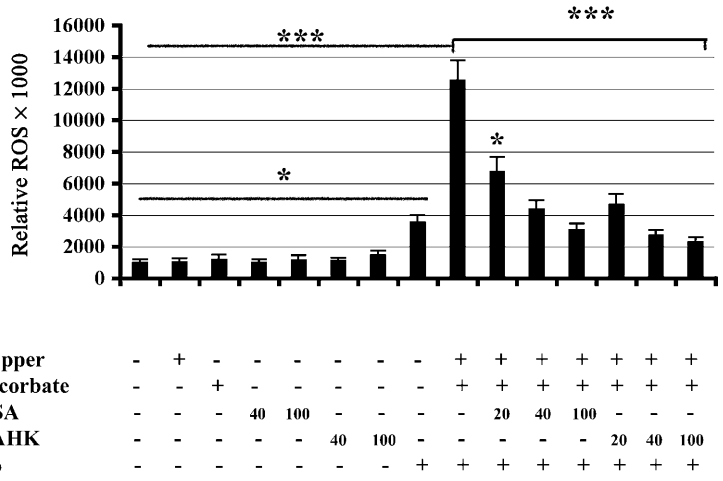

Figure 8. Effect of Cu^{II}–Aβ40 in the presence of ascorbate, DAHK and HSA on intracellular early ROS production in SH-SY5Y cells measured by using DCF fluorescence. Cells were treated as indicated in the Experimental Section. The intracellular production of ROS is significantly increased in the presence of the mixture Aβ, Cu, and ascorbate compared the controls (on the left, corresponding to untreated cells, Aβ, Cu, ascorbate, HSA, DAHK alone); *** = $p < 0.001$ (Aβ + Cu + ascorbate vs. control, Aβ, Cu, ascorbate, HSA and DAHK). ROS production is significantly decreased by the addition of HSA and DAHK at every concentration tested when compared to the levels produced by the mixture Aβ, Cu, and ascorbate; *** = $p < 0.001$ (Aβ + Cu + ascorbate vs. Aβ + Cu + ascorbate + HSA or DAHK at every condition tested. ROS production produced by the mixture Aβ, Cu, ascorbate, and 20 μM HSA is significantly increased compared to ROS production by Aβ alone; * = $p < 0.05$ (Aβ + Cu + ascorbate + HSA 20 μM vs. Aβ. Addition of HSA at 40 and 100 mM or DAHK at 20, 40, and 100 mM to the mixture Aβ + Cu + ascorbate is not significantly different compared to Aβ alone in the absence of Cu and ascorbate. Conditions: Aβ 40 μM, Cu 40 μM, ascorbate 300 μM, DAHK and HSA 20, 40 or 100 μM as indicated. $n = 18$ from three independent experiments.

Discussion

The present work suggests that HSA is a much stronger Cu^{II} chelator than Aβ (about $\geq$100 times) and is hence able to retrieve Cu^{II} from Aβ efficiently and rapidly (few seconds or faster). Considering the plasma concentrations of 0.6 mM for HSA and about 0.5 nM for Aβ, almost no Cu^{II} copper should be bound to Aβ. Consequently, HSA can be considered as a native protein attenuating the aberrant Cu^{II} binding to Aβ, and Cu binding to Aβ in the blood plasma is likely not of physiological relevance under normal conditions.

Similar suggestions can be made for the CSF, where concentrations of HSA and Aβ have been reported.[28,45] In this fluid the concentration ratio of Aβ to HSA is increased compared to the blood, as Aβ is higher (~10–100×) but HSA is lower (~100×). Despite the ratio's being favourable for Cu bound to Aβ, the distribution under these conditions would not exceed 0.1% of Cu bound to Aβ (compared to >99.9% on HSA). HSA is hence potentially able, also in the CSF, to attenuate aberrant copper(II) binding to Aβ. Since Cu–HSA does produce much less HO• than Cu–Aβ in the presence of ascorbate and HSA can decrease Cu^{II}-induced Aβ aggregation, HSA can be considered to be a physiological protector against Cu–Aβ toxicity. More Cu bound to Aβ is expected in Alzheimer's disease patients, where Aβ and extracellular copper concentrations increase, and the BBB penetration of HSA diminishes.[2,5]

However, these considerations are limited since several parameters are not known: 1) the Cu load of HSA in the CSF: as the brain has higher total Cu concentrations than the plasma it is possible that the occupancy of the high affinity N-terminal Cu site in HSA is higher than the few percent in the blood plasma; 2) the concentrations of Aβ and HSA in the brain apart from the CSF: in particular, the concentrations in the synaptic cleft would be important, as this is a pivotal location for the Aβ toxicity and plaque formation; and 3) importantly the redox state of the Cu (Cu^{II} vs. Cu^{I}) has not been identified.

The Cu redox state could explain why HSA and DAHK were able to rescue cells only partially from toxicity of Cu–Aβ in the presence of ascorbate. The reduction of Cu^{II} to Cu^{I} in the cell culture medium by

ascorbate and subsequent release of the Cu^{I} from HSA to another ligand is conceivable, as Cu^{I} prefers a tetrahedral coordination and sulfur ligands, and hence has a relatively low affinity of Cu^{I} to the square planar ATCUN motif. In the in vitro measurement of $HO^{\bullet}$ production, Cu^{I} might still be bound to HSA/DAHK, because no competing ligand is present.[23] In contrast, competing ligands are present in the cell culture medium or at the cell membrane.[2]

In the framework of using chelators as for Alzheimer's therapy (MPAC) the idea is to withdraw copper from aberrant interaction with Aβ and prevent, as such, ROS production by Cu–Aβ. However, a prerequisite is that the complex of metal and chelator (MPAC) itself does not produce oxidative stress, hence in the case of copper, the Cu–MPAC complex should not be redox active under physiological conditions. This can be achieved by either stabilizing Cu in its reduced Cu^{I} or in its oxidized Cu^{II} state in order to impede Cu redox cycling. HSA is able to stabilize the Cu^{II} state and hence suppressed $HO^{\bullet}$ almost completely, but not totally. DAHK was even more efficient due to an unknown mechanism. It is possible that in HSA an additional amino acid is coordinating Cu^{II}, in the axial position, that facilitates the reduction of Cu^{II} by ascorbate. Another possibility would be that HSA possesses a Cu^{I}-binding site distinct from the N-terminal ATCUN. This could be one of the other metal sites of HSA.[33,70] This suggests that Cu^{II}–MPAC complexes should have a low redox potential, preferentially even lower than DAHK.[23] Because the brain is a relatively reducing environment (even extracellularly due to hundreds of μM ascorbate[63]) the strategy of using a redox-inert Cu^{I} chelator instead of a redox-inert Cu^{II} chelator might be even more promising, as suggests the higher protection of MT-3 compared to HSA.[64]

In conclusion, the present data show that HSA and its isolated N-terminal Cu-binding peptide, DAHK, are much stronger Cu^{II} chelators than Aβ. HSA/DAHK can withdraw Cu^{II} from Aβ quantitatively and rapidly. Moreover, HSA and DAHK were able to decrease Cu-induced aggregation, and to suppress Cu–Aβ induced ROS production in the presence of ascorbate in vitro and in cell culture. Thus, HSA is a native protein able to function as metal–protein attenuating compound (MPAC) by reducing the aberrant Cu–Aβ interaction. This is very likely to happen in the blood plasma, where Cu is in the Cu^{II} state. However, this is less clear for the more reducing environment found in the brain, because HSA might be a less potent MPAC when copper is in the redox state Cu^{I}. Copper(I) chelators, such as the native protein MT-3, could be more potent under reducing conditions.

Experimental Section

Peptides and sample preparation: Aβ40 (Asp-Ala-Glu-Phe-Arg-His-Asp-Ser-Gly-Tyr-Glu-Val-His-His-Gln-Lys-Leu-Val-Phe-Phe-Ala-Glu-Asp-Val-Gly-Ser-Asn-Lys-Gly-Ala-Ile-Ile-Gly-Leu-Met-Val-Gly-Gly-Val-Val) and Aβ16 (amino acids 1–16) were purchased from EZBiolab (Westfield, IN, USA), Geneshere Biotechnologies (Paris, France) or Activotec (Cambridge, UK). ESI-MS of Aβ16 and Aβ40 showed masses of the monocharged species, which were within ±0.3 units from calculated masses. Stock solutions were prepared by dissolving the peptides in water. Aβ40 was incubated for 1 min at pH 10–11 to monomerise it. Then the pH was adjusted to 7.4 by adding buffer and HCl. The peptide concentrations of Aβ16 and Aβ40 were determined by absorption spectroscopy by using the extinction coefficient of Tyr at 276 nm, $\varepsilon = 1410\ cm^{-1}\,M^{-1}$.

The peptide DAHK (Asp-Ala-His-Lys) was purchased from Bachem. The stock solutions were prepared by dissolving the appropriate mass of peptide in water to obtain a concentration of 0.1 M. The concentration was confirmed by titration with Cu^{II}, based on the knowledge that DAHK can bind 1 equiv of Cu^{II} with the typical absorption maximum at 520 nm. The stock solutions were stored at −20 °C.

A stock solution (1 mM) of deferoxamine (Sigma) was prepared by dissolving the appropriate mass of deferoxamine powder in phosphate (20 mM), NaCl (100 mM) buffer (PBS) at pH 7.4 at room temperature. This stock solution was stored at −20 °C.

A stock solution (10 mM) of ascorbic acid was prepared in phosphate (20 mM), NaCl (100 mM) buffer (PBS) at pH 7.4 at room temperature just before beginning the experiment and was used immediately. Since ascorbate degrades very quickly, a new solution was prepared for each experiment.

Essentially fatty acid free HSA was used (Sigma) without further purification. HSA concentrations were determined by using an extinction coefficient at 280 nm of $33000\ cm^{-1}\,M^{-1}$.[71] About 0–10% of the N terminus of HSA is normally truncated and hence Cu binding to this site is abolished.[72] Thus the concentration of N-terminal Cu-binding site was measured by titrating Cu^{II} to HSA, based on the knowledge that the intact N terminus of HSA can bind 1 equiv Cu^{II} with the typical absorption maximum at 520 nm (further addition of Cu^{II} gives absorption at around 600 nm). For the rest of the experiments the concentration of HSA refers to the concentration of HSA with an intact N terminus.

Cu^{II} was generally added from a stock solution of $CuCl_2$ (Sigma) at slightly substoichiometric levels (0.9 equiv) to ensure total binding of Cu^{II} to the peptides/proteins. However, several control experiments with 1.0 equiv Cu^{II} showed no significant difference

Measurements of $HO^{\bullet}$: Measurements of $HO^{\bullet}$ production and detection by the Cu–peptides were performed in phosphate (20 mM), NaCl (100 mM) buffer (PBS) at pH 7.4. The Cu concentration was 10 or 80 μM. Peptide/protein was added slightly over-stoichiometrically (1.2–1.3 equiv) to ensure total binding of Cu^{II}. The relative $HO^{\bullet}$ generation between the different Cu complexes was similar at 10 and 80 μM. The reaction was started by the addition of either 300 or 600 μM ascorbate. In all these experiments, deferoxamine (final concentration 1 μM) was added to suppress $HO^{\bullet}$ generation of Fe as described earlier.[23] Deferoxamine (1 μM) was sufficient to abolish $HO^{\bullet}$ generation by the trace metals in the buffer. Deferoxamine might also chelate a part of the copper added (10 μM) if the traces of metals in buffer are overestimated, but this cannot exceed 10%. Although this adds uncertainty of up 1 μM Cu bound to the peptides, it does not change the general conclusions.

Size-exclusion chromatography: SEC of the peptides was performed at room temperature on a Superdex 75 10/300 GL column with an AKTA instrument (Amersham Pharmacia Biotech) under isocratic condition. Absorption was recorded at wavelengths of 275, 520 and 600 nm. The calibration of the column was performed

[2] *Stronger Cu^{I} ligands than HSA in the cell culture medium would also facilitate the reduction by ascorbate of DAHK, which was not reduced in the absence of other ligands (Figure 7).*

as described previously.[18] After equilibrating the column with elution buffer (PBS; flow rate: 0.8 mL min^{-1}), peptide samples (100 μL) were injected. The Cu content of Aβ and HSA/DAHK was estimated by the peak height of the d–d transitions by using the extinction coefficient of 60 cm^{-1} M^{-1} at 600 nm and of 100 cm^{-1} M^{-1} at 520 nm, respectively.[33,59] HSA eluted with two peaks: a major peak at about 9.4 mL corresponding to the monomer, and a minor peak at ~8.2 mL corresponding to the dimer; Aβ monomers eluted at 13.5 mL.[18]

Transmission electron microscopy: Peptide samples (5 μL) were applied on EM grids, washed with MilliQ water (5 μL) and negatively stained with an aqueous solution of uranyl acetate (5 μL; 1%, *w/w*). Samples were air-dried and examined with a JEOL 1011 transmission electron microscope operating at an accelerating voltage of 100 kV.

Absorption spectroscopy: UV/Vis absorption spectra were recorded at room temperature on a diode array spectrometer (HP 8453 E, Agilent) in a 1 cm path length quartz cuvette. UV absorption was used to determine the concentration of peptide Aβ16 and Aβ40. Turbidity was measured at 400 nm.

Fluorescence spectroscopy: Fluorescence spectra were collected by using a FLX-Spectrofluorimeter (Safas, Monaco) in 96-wells plates (final sample volume 200 μL). Coumarin-3 carboxylic acid (3-CCA; Sigma) was used to detect hydroxyl radicals (HO$^{\bullet}$) in PBS buffer.[23] HO$^{\bullet}$ reacts with 3-CCA to give 7-OH-CCA, which is fluorescent at 452 nm upon excitation at 395 nm. Samples were placed in a four-sided quartz fluorescence cuvette and data were recorded at room temperature. A solution of 3-CCA (1 mM) was prepared in phosphate (20 mM), NaCl (100 mM) buffer (PBS) at pH 7.4 at room temperature.

EPR spectroscopy: X-band EPR data were recorded by using an Elexsys ESP 500 operating at a microwave frequency of ~9.5 GHz. For the titration of Cu–Aβ with HSA, the spectra were recorded at 100 K by using a nitrogen gas flow with a microwave power of 20 mW and modulation amplitude of 10 Gauss. Prior to measurements, the samples were mixed with glycerol (10%, *v/v*) to obtain homogeneous freezing.

Cell viability assay (MTT): Human neuroblastoma SH-SY5Y cells (DSMZ, Germany) were grown for two days in DMEM medium (Gibco, Invitrogen) with foetal calf serum (FCS; 10%; Hyclone, Inc.), L-glutamine (0.2 mM) and gentamycin (0.5%; Eurobio) at 37 °C in a humidified atmosphere with 5% CO_2. To assess the effects of HSA or DAHK on Cu–Aβ40 induced toxicity, cells were seeded at a 2×10^5 cells per well density in 24-well plates in PBS containing DMEM (10%; without FCS) and then exposed for 24 h to freshly prepared Cu^{II}–Aβ40 (40 μM) in the presence of different concentrations of either HSA or DAHK (0, 40 or 100 mM) with ascorbate (300 mM). As a control, cells were grown with and without Cu^{II}–Aβ40. Cell viability was measured by using the 3-(4,5-dimethylthiazol-2-yl)-2,5-diphenyltetrazolium bromide (MTT) dye reduction assay as described previously.[73] Basically, MTT (25 μL of 5 mg mL^{-1} solution in PBS) was added to each well (24-well plate containing 500 μL medium) and incubated for 3 h. Subsequently, DMSO (1 mL) was added and the reduced MTT was measured by absorption at 570 nm. Results are the average of three independent experiments following normalization ($n=3$).

Determination of intracellular ROS levels: Cells were plated on 96-wells plates. The day before experiments, SH-SY5Y cells were cultured in medium containing 2% FCS (Gibco) and maintained in low serum condition for 16 h. The day of the experiments, cells were washed with PBS and incubated in 5% CO_2/95% air at 37 °C for 6 h in DMEM without FCS. Cells were washed twice with DMEM. Aβ peptide (40 mM) was preincubated 5 min at room temperature in DMEM containing copper (40 mM) and ascorbate (300 mM), with either HSA or DAHK (0, 20, 40, or 100 mM) in a final volume of 50 μL. The cells were treated with the different mixtures for 20 min at 37 °C.

Intracellular ROS levels were monitored by using the fluorescent dye 2′,7′-dichlorodihydrofluorescein diacetate (H_2DCFDA; Molecular-Probes, Invitrogen) as previously described.[74] After treatment, cells were washed twice and incubated in DMEM containing H_2DCFDA (20 μM). After 30 min incubation at 37 °C, cells were washed with PBS and fluorescence intensity was measured in a Fluoro plate reader (FLX800 Biotek Instruments, software KL4) with the excitation and emission wavelengths at (485 ± 20) nm and (525 ± 20) nm, respectively. The cell-permeant H_2DCFDA is converted into a nonfluorescent polar derivative (H_2DCF) by cellular esterases after incorporation into cells. H_2DCF is oxidized rapidly to the highly fluorescent 2′,7′-dichlorofluorescein (DCF) in the presence of intracellular ROS. The results obtained are the average of three independent experiments each of them performed with six replicates for each point analyzed ($n=18$ and three independent experiments).

Statistical analysis on cellular experiments: The statistical significance of differences between the means was evaluated by one-way analysis of variance (ANOVA). Calculations were done by using Instat (GraphPad software).

Acknowledgements

We thank Prof. Dr. Milan Vasak (University of Zürich) for providing MT-3, Vincent Collière for the TEM images and Lionel Rechignat for the EPR measurements, Dr. Vanessa Sonois for help with the cell culture experiments and Dr. Olivier Cuvillier (IPBS, Toulouse) for performing the statistical analysis. C.F. was supported from the US/France REU program. M.L.M. laboratory is supported by the ATIP program "Relations Structure-Fonction" of CNRS Life Science department and by the Foundation for Medical Research (FRM). This research was supported by a Marie-Curie International Reintegration grant number 224892, within the 7th European Community Framework Program to L.P. and M.L.M.

Keywords: amyloid beta-peptides · bioinorganic chemistry · copper · human serum albumin · reactive oxygen species

[1] D. J. Selkoe, *Science* **2002**, *298*, 789–791.
[2] M. Goedert, M. G. Spillantini, *Science* **2006**, *314*, 777–781.
[3] M. P. Mattson, *Nature* **2004**, *430*, 631–639.
[4] J. Hardy, D. J. Selkoe, *Science* **2002**, *297*, 353–356.
[5] D. J. Selkoe, *Physiol. Rev.* **2001**, *81*, 741–766.
[6] W. L. Klein, W. B. Stine, Jr., D. B. Teplow, *Neurobiol. Aging* **2004**, *25*, 569–580.
[7] P. J. Crouch, S. M. Harding, A. R. White, J. Camakaris, A. I. Bush, C. L. Masters, *Int. J. Biochem. Cell Biol.* **2008**, *40*, 181–198.
[8] P. A. Adlard, A. I. Bush, *J. Alzheimer's Dis.* **2006**, *10*, 145–163.
[9] D. G. Smith, R. Cappai, K. J. Barnham, *Biochim. Biophys. Acta* **2007**, *1768*, 1976–1990.
[10] X. Huang, C. S. Atwood, M. A. Hartshorn, G. Multhaup, L. E. Goldstein, R. C. Scarpa, M. P. Cuajungco, D. N. Gray, J. Lim, R. D. Moir, R. E. Tanzi, A. I. Bush, *Biochemistry* **1999**, *38*, 7609–7616.

[11] M. A. Lovell, J. D. Robertson, W. J. Teesdale, J. L. Campbell, W. R. Markesbery, *J. Neurol. Sci.* **1998**, *158*, 47 – 52.
[12] L. M. Miller, Q. Wang, T. P. Telivala, R. J. Smith, A. Lanzirotti, J. Miklossy, *J. Struct. Biol.* **2006**, *155*, 30 – 37.
[13] J. Dong, C. S. Atwood, V. E. Anderson, S. L. Siedlak, M. A. Smith, G. Perry, P. R. Carey, *Biochemistry* **2003**, *42*, 2768 – 2773.
[14] L. Q. Hatcher, L. Hong, W. D. Bush, T. Carducci, J. D. Simon, *J. Phys. Chem. B* **2008**, *112*, 8160 – 8164.
[15] P. Faller, C. Hureau, *Dalton Trans.* **2009**, 1080 – 1094.
[16] C. S. Atwood, R. D. Moir, X. Huang, R. C. Scarpa, N. M. Bacarra, D. M. Romano, M. A. Hartshorn, R. E. Tanzi, A. I. Bush, *J. Biol. Chem.* **1998**, *273*, 12817 – 12826.
[17] X. Huang, M. P. Cuajungco, C. S. Atwood, M. A. Hartshorn, J. D. A. Tyndall, G. R. Hanson, K. C. Stokes, M. Leopold, G. Multhaup, L. E. Goldstein, R. C. Scarpa, A. J. Saunders, J. Lim, R. D. Moir, C. Glabe, E. F. Bowden, C. L. Masters, D. P. Fairlie, R. E. Tanzi, A. I. Bush, *J. Biol. Chem.* **1999**, *274*, 37111 – 37116.
[18] C. Talmard, L. Guilloreau, Y. Coppel, H. Mazarguil, P. Faller, *ChemBioChem* **2007**, *8*, 163 – 165.
[19] J. W. Karr, V. A. Szalai, *Biochemistry* **2008**, *47*, 5006 – 5016.
[20] J. W. Karr, L. J. Kaupp, V. A. Szalai, *J. Am. Chem. Soc.* **2004**, *126*, 13534 – 13538.
[21] C. Sarell, C. Syme, S. Rigby, J. Viles, *Biochemistry* **2009**, *48*, 4388 – 4402.
[22] S. C. Drew, C. J. Noble, C. L. Masters, G. R. Hanson, K. J. Barnham, *J. Am. Chem. Soc.* **2009**, *131*, 1195 – 1207.
[23] L. Guilloreau, S. Combalbert, A. Sournia-Saquet, H. Marzaguil, P. Faller, *ChemBioChem* **2007**, *8*, 1317 – 1325.
[24] C. Opazo, X. Huang, R. A. Cherny, R. D. Moir, A. E. Roher, A. R. White, R. Cappai, C. L. Masters, R. E. Tanzi, N. C. Inestrosa, A. I. Bush, *J. Biol. Chem.* **2002**, *277*, 40302 – 40308.
[25] T. Kowalik-Jankowska, M. Ruta, K. Wisniewska, L. Lankiewicz, M. Dyba, *J. Inorg. Biochem.* **2004**, *98*, 940 – 950.
[26] S. I. Dikalov, M. P. Vitek, R. P. Mason, *Free Radical Biol. Med.* **2004**, *36*, 340 – 347.
[27] C. Hureau, P. Faller, *Biochimie* **2009**, *91*, 1212 – 1217.
[28] H. Reiber, *Clin. Chim. Acta* **2001**, *310*, 173 – 186.
[29] J. P. Laussac, B. Sarkar, *Biochemistry* **1984**, *23*, 2832 – 2838.
[30] W. Goumakos, J. P. Laussac, B. Sarkar, *Biochem. Cell Biol.* **1991**, *69*, 809 – 820.
[31] W. Bal, J. Christodoulou, P. J. Sadler, A. Tucker, *J. Inorg. Biochem.* **1998**, *70*, 33 – 39.
[32] P. J. Sadler, J. H. Viles, *Inorg. Chem.* **1996**, *35*, 4490 – 4496.
[33] E. Mothes, P. Faller, *Biochemistry* **2007**, *46*, 2267 – 2274.
[34] J. Masuoka, J. Hegenauer, B. R. Van Dyke, P. Saltman, *J. Biol. Chem.* **1993**, *268*, 21533 – 21537.
[35] M. Rozga, M. Sokolowska, A. M. Protas, W. Bal, *J. Biol. Inorg. Chem.* **2007**, *12*, 913 – 918.
[36] C. Harford, B. Sarkar, *Acc. Chem. Res.* **1997**, *30*, 123 – 130.
[37] W. Bal, M. I. Djuran, D. W. Margerum, E. T. J. Gray, M. A. Mazid, R. T. Tom, E. Nierboer, P. J. Sadler, *J. Chem. Soc. Chem. Commun.* **1994**, *16*, 1889 – 1990.
[38] M. C. Linder, L. Wooten, P. Cerveza, S. Cotton, R. Shulze, N. Lomeli, *Am. J. Clin. Nutr.* **1998**, *67*, 965S – 971S.
[39] J. F. Poduslo, G. L. Curran, C. T. Berg, *Proc. Natl. Acad. Sci. USA* **1994**, *91*, 5705 – 5709.
[40] R. W. Colburn, J. W. Maas, *Nature* **1965**, *208*, 37 – 41.
[41] E. T. Gum, R. A. Swanson, C. Alano, J. Liu, S. Hong, P. R. Weinstein, S. S. Panter, *Stroke* **2004**, *35*, 590 – 595.
[42] A. L. Biere, B. Ostaszewski, E. R. Stimson, B. T. Hyman, J. E. Maggio, D. J. Selkoe, *J. Biol. Chem.* **1996**, *271*, 32916 – 32922.
[43] M. Rozga, M. Kloniecki, A. Jablonowska, M. Dadlez, W. Bal, *Biochem. Biophys. Res. Commun.* **2007**, *364*, 714 – 718.
[44] B. Bohrmann, L. Tjernberg, P. Kuner, S. Poli, B. Levet-Trafit, J. Naslund, G. Richards, W. Huber, H. Dobeli, C. Nordstedt, *J. Biol. Chem.* **1999**, *274*, 15990 – 15995.
[45] R. Deane, Z. Wu, B. V. Zlokovic, *Stroke* **2004**, *35*, 2628 – 2631.
[46] J. F. Poduslo, G. L. Curran, T. M. Wengenack, B. Malester, K. Duff, *Neurobiol. Dis.* **2001**, *8*, 555 – 567.
[47] R. A. Cherny, C. S. Atwood, M. E. Xilinas, D. N. Gray, W. D. Jones, C. A. McLean, K. J. Barnham, I. Volitakis, F. W. Fraser, Y. Kim, X. Huang, L. E. Goldstein, R. D. Moir, J. T. Lim, K. Beyreuther, H. Zheng, R. E. Tanzi, C. L. Masters, A. I. Bush, *Neuron* **2001**, *30*, 665 – 676.
[48] P. A. Adlard, R. A. Cherny, D. I. Finkelstein, E. Gautier, E. Robb, M. Cortes, I. Volitakis, X. Liu, J. P. Smith, K. Perez, K. Laughton, Q. X. Li, S. A. Charman, J. A. Nicolazzo, S. Wilkins, K. Deleva, T. Lynch, G. Kok, C. W. Ritchie, R. E. Tanzi, R. Cappai, C. L. Masters, K. J. Barnham, A. I. Bush, *Neuron* **2008**, *59*, 43 – 55.
[49] L. Lannfelt, K. Blennow, H. Zetterberg, S. Batsman, D. Ames, J. Harrison, C. L. Masters, S. Targum, A. I. Bush, R. Murdoch, J. Wilson, C. W. Ritchie, *Lancet Neurol.* **2008**, *7*, 779 – 786.
[50] J. Y. Lee, J. E. Friedman, I. Angel, A. Kozak, J. Y. Koh, *Neurobiol. Aging* **2004**, *25*, 1315 – 1321.
[51] C. Boldron, I. Van der Auwera, C. Deraeve, H. Gornitzka, S. Wera, M. Pitie, F. Van Leuven, B. Meunier, *ChemBioChem* **2005**, *6*, 1976 – 1980.
[52] P. J. Crouch, L. W. Hung, P. A. Adlard, M. Cortes, V. Lal, G. Filiz, K. A. Perez, M. Nurjono, A. Caragounis, T. Du, K. Laughton, I. Volitakis, A. I. Bush, Q. X. Li, C. L. Masters, R. Cappai, R. A. Cherny, P. S. Donnelly, A. R. White, K. J. Barnham, *Proc. Natl. Acad. Sci. USA* **2009**, *106*, 381 – 386.
[53] G. Rakhit, W. E. Antholine, W. Froncisz, J. S. Hyde, J. R. Pilbrow, G. R. Sinclair, B. Sarkar, *J. Inorg. Biochem.* **1985**, *25*, 217 – 224.
[54] G. Rakhit, B. Sarkar, *J. Inorg. Biochem.* **1981**, *15*, 233 – 241.
[55] C. C. Curtain, F. Ali, I. Volitakis, R. A. Cherny, R. S. Norton, K. Beyreuther, C. J. Barrow, C. L. Masters, A. I. Bush, K. J. Barnham, *J. Biol. Chem.* **2001**, *276*, 20466 – 20473.
[56] M. Sokolowska, A. Krezel, M. Dyba, Z. Szewczuk, W. Bal, *Eur. J. Biochem.* **2002**, *269*, 1323 – 1331.
[57] T. Kowalik-Jankowska, M. Ruta, K. Wisniewska, L. Lankiewicz, *J. Inorg. Biochem.* **2003**, *95*, 270 – 282.
[58] C. D. Syme, R. C. Nadal, S. E. Rigby, J. H. Viles, *J. Biol. Chem.* **2004**, *279*, 18169 – 18177.
[59] L. Guilloreau, L. Damian, Y. Coppel, H. Mazarguil, M. Winterhalter, P. Faller, *J. Biol. Inorg. Chem.* **2006**, *11*, 1024 – 1038.
[60] J. Milojevic, V. Esposito, R. Das, G. Melacini, *J. Am. Chem. Soc.* **2007**, *129*, 4282 – 4290.
[61] D. P. Smith, G. D. Ciccotosto, D. J. Tew, M. T. Fodero-Tavoletti, T. Johanssen, C. L. Masters, K. J. Barnham, R. Cappai, *Biochemistry* **2007**, *46*, 2881 – 2891.
[62] A. I. Bush, *Trends Neurosci.* **2003**, *26*, 207 – 214.
[63] M. E. Rice, *Trends Neurosci.* **2000**, *23*, 209 – 216.
[64] G. Meloni, V. Sonois, T. Delaine, L. Guilloreau, A. Gillet, J. Teissie, P. Faller, M. Vasak, *Nat. Chem. Biol.* **2008**, *4*, 366 – 372.
[65] R. C. Nadal, S. E. Rigby, J. H. Viles, *Biochemistry* **2008**, *47*, 11653 – 11664.
[66] D. Bar-Or, L. T. Rael, E. P. Lau, N. K. Rao, G. W. Thomas, J. V. Winkler, R. L. Yukl, R. G. Kingston, C. G. Curtis, *Biochem. Biophys. Res. Commun.* **2001**, *284*, 856 – 862.
[67] G. Meloni, P. Faller, M. Vasak, *J. Biol. Chem.* **2007**, *282*, 16068 – 16078.
[68] A. Gomez-Brouchet, D. Pchejetski, L. Brizuela, V. Garcia, M. F. Altié, M. L. Maddelein, M. B. Delisle, O. Cuvillier, *Mol. Pharmacol.* **2007**, *72*, 341 – 349.
[69] A. Pensalfini, C. Cecchi, M. Zampagni, M. Becatti, F. Favilli, P. Paoli, S. Catarzi, S. Bagnoli, B. Nacmias, S. Sorbi, G. Liguri, *Free Radical Biol. Med.* **2008**, *44*, 1624 – 1636.
[70] A. J. Stewart, C. A. Blindauer, S. Berezenko, D. Sleep, P. J. Sadler, *Proc. Natl. Acad. Sci. USA* **2003**, *100*, 3701 – 3706.
[71] F. B. Edwards, R. B. Rombauer, B. J. Campbell, *Biochim. Biophys. Acta* **1969**, *194*, 234 – 245.
[72] D. Bar-Or, R. Bar-Or, L. T. Rael, D. K. Gardner, D. S. Slone, M. L. Craun, *Crit. Care Med.* **2005**, *33*, 1638 – 1641.
[73] O. Cuvillier, T. Levade, *Blood* **2001**, *98*, 2828 – 2836.
[74] A. Pines, L. Perrone, N. Bivi, M. Romanello, G. Damante, M. Gulisano, M. R. Kelley, F. Quadrifoglio, G. Tell, *Nucleic Acids Res.* **2005**, *33*, 4379 – 4394.

Received: July 30, 2009
Published online on November 24, 2009

